Supplemental Methods

In vitro mouse islets/islet cell culture, synchronization, and bioluminescence monitoring

For *in vitro* culture, the intact islets, dissociated or sorted cells were recovered in RPMI 1640 complete medium (11.2 mM glucose, 110 µg/mL sodium pyruvate) supplemented with 10 % fetal calf serum, 110 units/mL penicillin, 110 µg/mL streptomycin, and 50 µg/mL gentamycin and attached to 35 mm dishes or multi-well plates, pre-coated with a laminin-5-rich extracellular matrix (Parnaud et al., 2008). Adherent islets/cells were synchronized by a 1 h pulse of forskolin 10 µM (Sigma) prior to continuous bioluminescence recording in RPMI supplemented with 100 µM luciferin (NanoLight Technology). For detrended time series, raw luminescence signals were processed by a moving average with a window of 24 h (Petrenko et al., 2017).

Supplemental Figure Legends

Figure S1. Experimental outline. (A) Quintuple transgenic mice (*ProGcg-Venus*/RIP-*Cherry*/*Per2*::*Luc/rtTA/TET-DTA*) were kept at standard 12/12 h light-dark cycle conditions. Animals were subjected to night-restricted feeding two weeks prior to the islet collection and during the entire experiment time, with constant and unrestricted access to drinking water. Experimental animals (doxycycline, DOX group) received 300 µg/ml of doxycycline (DOX) in the drinking water supplemented with 2 % sucrose during the entire experiment time (7-10 days). Control animals (CTR) received drinking water supplemented with 2 % sucrose during the same period. ZT0 (*Zeitgeber*) corresponds to 7AM, the time of light switch-on in the animal facility, and ZT12 to 7PM, the time of light switch-off. Pancreatic islets were isolated between 12 and 14 days following DOX treatment, around-the-clock every 4 h during 24 h. Pancreatic islet isolation was performed from 2-4 animals per replicate in two independent experiments at each time point

(total of 4-8 animals per time point), with subsequent gently trypsinization and separation of α- and β-cells by FACS. RNA was extracted from two cell populations obtained at each time point and subjected to RNA sequencing (RNA-seq) and qPCR analyses. Blood sampling was conducted at the same time-points across 24 h to measure the blood levels of glucose, insulin, and glucagon. (B) Ratio (R) between FACS-separated α- and β-cells in control and DOX-treated groups. Data are expressed as mean ± SEM for n = 10 preparations. (C) Glycemic profile of mice at 7, 9, and 14 days following DOX treatment. (D) Proliferation of β-cells in response to massive ablation. The number of BrdU/Insulin double-positive cells within insulin-labeled population across all samples shown in Figure 1A (CTR and DOX group, 6 time-points per group, 3 mice per time-point, total of 36 samples). Data are expressed as mean ± SEM for n = 36 mice per phenotype. The difference was tested using Students t-test; ***$p<0.001$.

Figure S2. Enlarged split channel view of the confocal images of the islets from DOX-treated triple-DTA mice at ZT8 and ZT16 shown on Figure 1A. Localization of proliferation marker BrdU in insulin-producing β-cells is indicated by arrows. Scale bar = 50 μm.

Figure S3. Differential analysis of gene expression in α- and β-cells following massive β-cell ablation. (A, C) Volcano plots representing transcripts that were differentially expressed between α- and β-cells in CTR (A) and DOX (C) groups. For differential analysis, the average across 6 points per each of 4 conditions (α- and β-cells, treated or not with DOX) was considered. Upregulated genes are labeled in green; downregulated are in red. Size of dots corresponds to the Log_{10} p value. (B, E) Histograms presenting number of differentially expressed (up- and downregulated genes) between α- and β-cells in CTR (B) and DOX (E) groups at each of 6 time-points (see Figure S1A for experimental design). (D) KEGG pathway enrichment analysis of

differentially expressed transcripts between α- and residual β-cells after ablation showing significance (-log10 p-value, x-axis) for indicated pathway (y-axis).

Figure S4. Changes in core-clock machinery in residual β-cells following ablation. (A) Results of KEGG pathway enrichment analysis of β-cells transcripts that showed phase-difference between CTR and DOX groups of -2 and +2 h, with indicated significance (-log10 p-value, x-axis) for indicated pathway (y- axis). (B-C) Average PER2::Luc oscillation profiles of forskolin-synchronized islets (B, n = 4 independent experiments) and dispersed islet cells (n = 1 experiment, isolated from 3 mice) recorded with lumicycle. Data are presented as detrended values, obtained as described in details in (Pulimeno et al., 2013). (D-E) Temporal profiles of *MafA* (D) and *Wee1* (E) transcripts in sorted β-cells with and without DOX treatment. Data are expressed as mean ± SD for two experimental repetitions per each time-point, with at least 3 mice in each replicate.

Figure S5. RNAseq analysis of β-cells in *Bmal1*$^{st/st}$ mice following massive β-cell ablation. (A) Schematic representation of the *Bmal1* stop-cassette knock-in allele. SA, splice acceptor; 3xpA, triple repeat of a polyadenylation signal sequence; Triangles, *LoxP* sites. (B) Average PER2::Luc oscillation profiles of forskolin-synchronized islets isolated from *Bmal1*$^{st/st}$ and *Bmal1*$^{+/st}$ mice (n = 4 independent experiments) recorded with lumicycle. Data are presented as detrended values. (C) *Bmal1* (*Arntl*) gene reads coverage based on raw RNA-seq data, indicating weak reads coverage starting from the 5th exon in *Bmal1*$^{st/st}$DOX mice (labelled as *Bmal1*KO_DOX) as compared to heterozygotes counterparts (labelled as *Bmal1*Het_DOX). (D) IPA generated Top 5 canonical pathways based on differentially expressed genes between *Bmal1*$^{st/st}$DOX and *Bmal1*$^{+/st}$DOX mice. (E) IPA-generated Circadian Rhythm Canonical Pathway displaying core-clock components within circadian rhythm pathway differentially expressed between two groups. (F) Arntl (Bmal1)-centered IPA-generated top network based on RNA-seq differential expression

data (Dataset S7). (G) KEGG pathway enrichment analysis of differentially expressed transcripts between *Bmal1*$^{+/st}$DOX and *Bmal1*$^{st/st}$DOX residual β-cells after ablation showing significance (-log10 p-value, x-axis) for indicated pathway (y-axis).

Figure S6. Parameters of glucose metabolism in *Bmal1*$^{+/+}$ and *Bmal1*$^{+/st}$ mice. Assessment of blood glucose (A), insulin (B) and glucagon (C) levels in *Bmal1*$^{+/+}$ mice (*proGcg*-Venus/RIP-Cherry/PER2*::*L*uc*/*Insulin-rtTA/TET-DTA,* no DOX treatment) and in *Bmal1*$^{+/st}$ (*Bmal1*$^{+/st}$DTA, no DOX treatment) mice at ZT4. Data are expressed as Mean ± SEM for n = 8-18 mice per group. Student's t-test comparisons were applied, difference between groups was non-significant.

Figure S7. High resolution and split channel view of the representative confocal images of *Bmal1*$^{st/st}$DOX and *Bmal1*$^{+/st}$DOX islets shown on Figure 5B. Localization of proliferation marker BrdU in insulin-producing β-cells is indicated by arrows. Scale bar = 50 μm.

Figure S8. Workflow of RNA-seq data analyses presented in Figures 2, 3 and 6.

Supplemental Table S1. Sequences of quantitative RT-PCR primers

Target gene		*Sequence primers*
mAurkB	*forward*	5'-TCGGGGTGCTCTGCTATGAA -3'
	reverse	5'-CCACCTTGACAATCCGACGA -3'
mPappa2	*forward*	5'-CAGCCCTTGTCATTGACTGTG T -3'
	reverse	5'-AGCAACCCAGCCATCATTG -3'
mMafA	*forward*	5'-CATTCTGGAGAGCGAGAAGTG-3'
	reverse	5'-TTTCTCCTTGTACAGGTCCCG -3'
mKi67	*forward*	5'-CTGCCTGCGAAGAGAGCATC -3'
	reverse	5'-AGCTCCACTTCGCCTTTTGG -3'
mS9	*forward*	5'-CTCCGGAACAAACGTGAGGT-3'

	reverse	5’-TCCAGCTTCATCTTGCCCTC -3’
mHprt	*forward*	5’-GATTTTATCAGACTGAAGAGC-3’
	reverse	5’-TCCAGTTAAAGTTGAGAGAGATC -3’

Supplemental Datasets

Dataset S1. List of differentially expressed genes (related to Figure 2, Figure S3).

Dataset S2. Gene distribution within the rhythmicity models between control α- and control β-cells (related to Figure 3).

Dataset S3. Gene distribution within the rhythmicity models between control and DOX treated β-cells (related to Figure 3).

Dataset S4. Gene distribution within the rhythmicity models between DOX treated α- and β-cells (related to Figure 3).

Dataset S5. Gene distribution within the rhythmicity models between control and DOX treated α-cells (related to Figure 3).

Dataset S6. Circadian rhythmic genes exhibiting phase shift in different conditions and cells.

Dataset S7. List of differentially expressed genes between β-cells from *Bmal1*$^{st/st}$ and *Bmal1*$^{+/st}$ mice treated with DOX.

Dataset S8. List of differentially expressed genes between β-cells from *Bmal1*$^{st/st}$ treated with DOX or untreated controls.

Dataset S9. List of the genes selected for the algorithm entrainment.

References

Parnaud, G., Bosco, D., Berney, T., Pattou, F., Kerr-Conte, J., Donath, M.Y., Bruun, C., Mandrup-Poulsen, T., Billestrup, N., and Halban, P.A. (2008). Proliferation of sorted human and rat beta cells. Diabetologia *51*, 91-100.

Petrenko, V., Gosmain, Y., and Dibner, C. (2017). High-Resolution Recording of the Circadian Oscillator in Primary Mouse alpha- and beta-Cell Culture. Front Endocrinol (Lausanne) *8*, 68.

Pulimeno, P., Mannic, T., Sage, D., Giovannoni, L., Salmon, P., Lemeille, S., Giry-Laterriere, M., Unser, M., Bosco, D., Bauer, C., et al. (2013). Autonomous and self-sustained circadian oscillators displayed in human islet cells. Diabetologia *56*, 497-507.

A

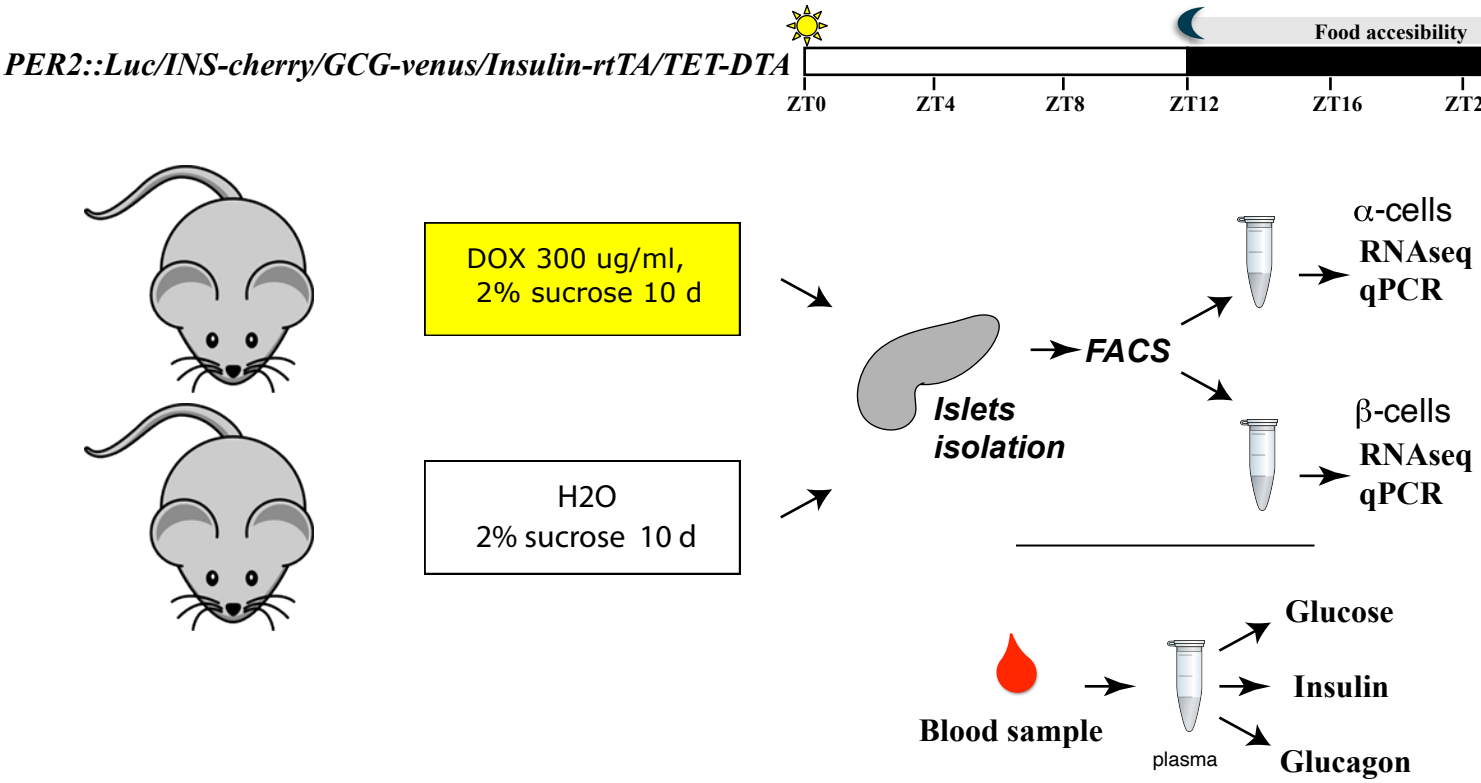
MODEL
SAMPLING
PER2::Luc/INS-cherry/GCG-venus/Insulin-rtTA/TET-DTA
Food accesibility
ZT0
ZT4
ZT8
ZT12
ZT16
ZT20
DOX 300 ug/ml,
2% sucrose 10 d
H2O
2% sucrose 10 d
Islets
isolation
FACS
α-cells
RNAseq
qPCR
β-cells
RNAseq
qPCR
Blood sample
plasma
Glucose
Insulin
Glucagon

B

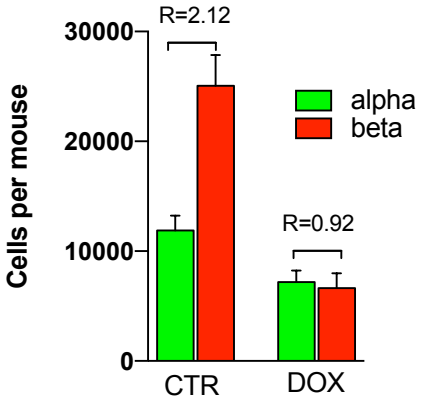
R=2.12
30000
20000
10000
0
Cells per mouse
alpha
beta
R=0.92
CTR
DOX

C

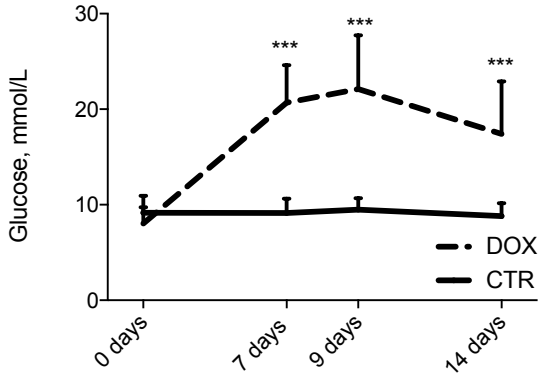
30
20
10
0
Glucose, mmol/L
***
***
***
DOX
CTR
0 days
7 days
9 days
14 days

D

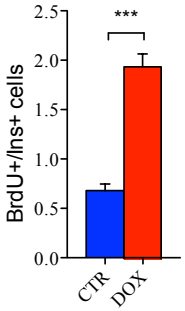
2.5
2.0
1.5
1.0
0.5
0.0
BrdU+/Ins+ cells
***
CTR
DOX

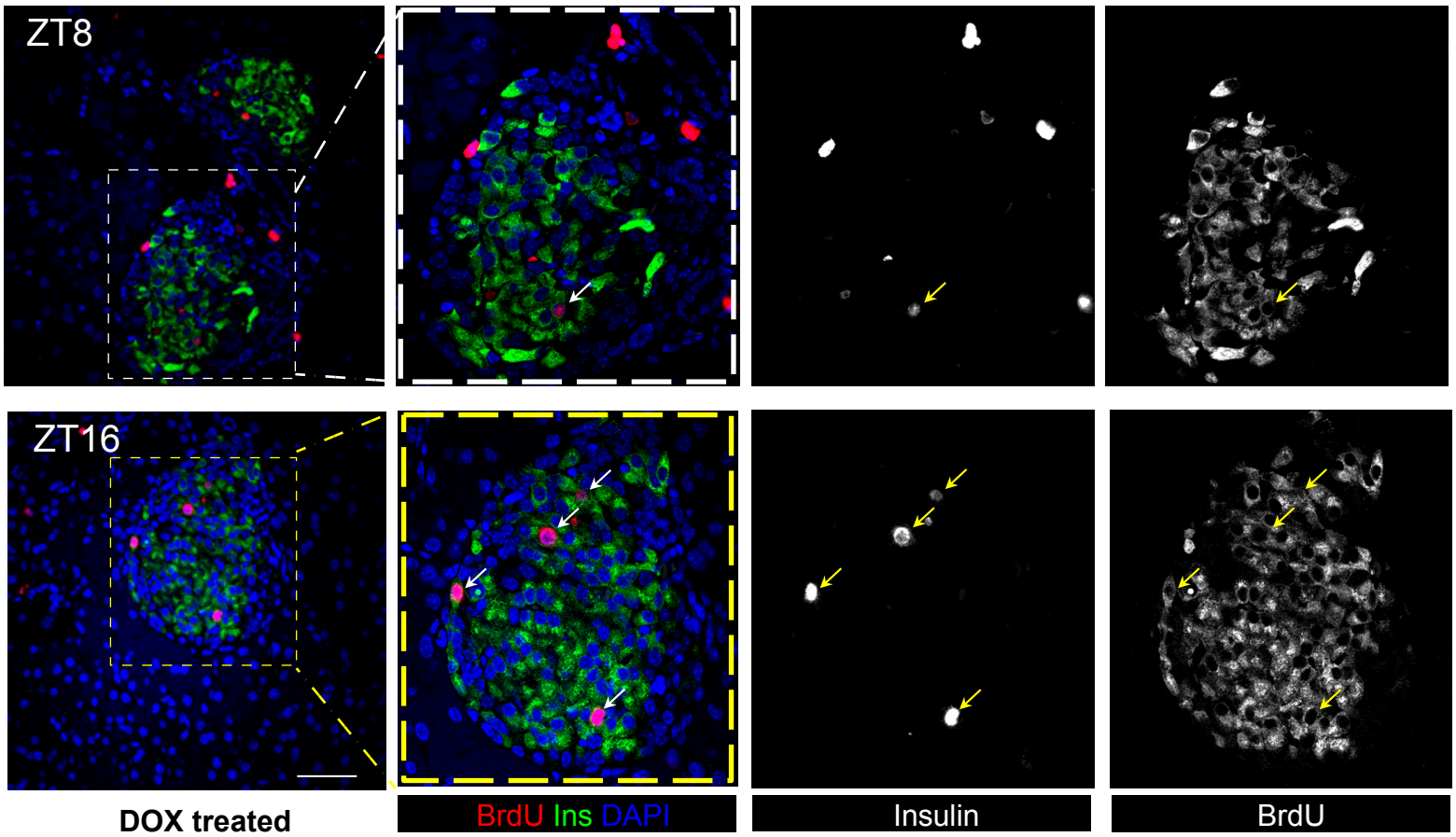
ZT8
ZT16
DOX treated
BrdU Ins DAPI
Insulin
BrdU

A

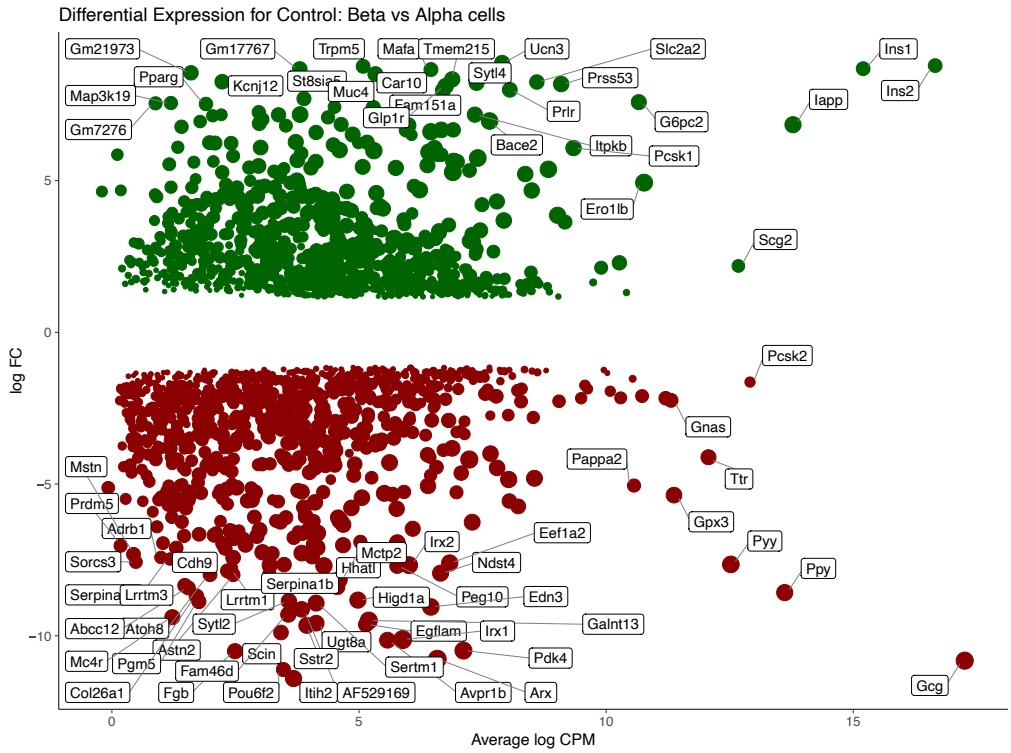
Differential Expression for Control: Beta vs Alpha cells
log FC
Average log CPM
Gm21973
Gm17767
Trpm5
Mafa
Tmem215
Ucn3
Slc2a2
Ins1
Pparg
Kcnj12
Car10
Sytl4
Prss53
Ins2
Map3k19
Muc4
Fam151a
Prlr
Iapp
Gm7276
Glp1r
G6pc2
Bace2
Itpkb
Pcsk1
Ero1lb
Scg2
Pcsk2
Gnas
Pappa2
Ttr
Mstn
Prdm5
Gpx3
Adrb1
Eef1a2
Pyy
Irx2
Mctp2
Sorcs3
Cdh9
Hhatl
Ndst4
Ppy
Serpina1b
Serpina
Lrrtm3
Lrrtm1
Higd1a
Peg10
Edn3
Abcc12
Atoh8
Sytl2
Egflam
Irx1
Galnt13
Ugt8a
Astn2
Scin
Sstr2
Pdk4
Mc4r
Pgm5
Fam46d
Sertm1
Col26a1
Fgb
Pou6f2
Itih2
AF529169
Avpr1b
Arx
Gcg

B

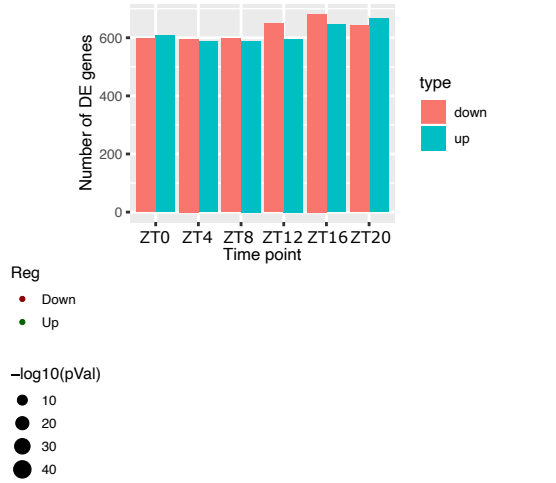
Type of test: CB_CA
Number of DE genes
Time point
ZT0
ZT4
ZT8
ZT12
ZT16
ZT20
type
down
up
Reg
Down
Up
−log10(pVal)
10
20
30
40

C

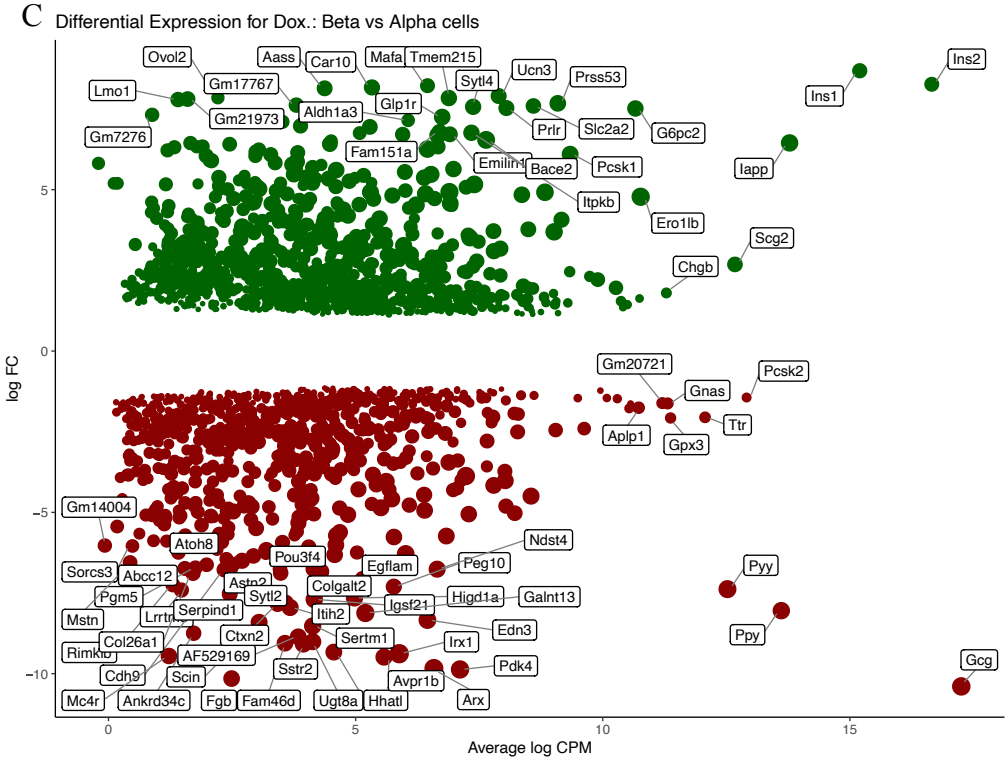
Differential Expression for Dox.: Beta vs Alpha cells
log FC
Average log CPM
Ovol2
Aass
Car10
Mafa
Tmem215
Ucn3
Ins2
Lmo1
Gm17767
Sytl4
Prss53
Ins1
Aldh1a3
Glp1r
Gm21973
Prlr
Slc2a2
G6pc2
Gm7276
Fam151a
Emilin1
Bace2
Pcsk1
Iapp
Itpkb
Ero1lb
Scg2
Chgb
Gm20721
Pcsk2
Gnas
Aplp1
Ttr
Gpx3
Gm14004
Atoh8
Ndst4
Pou3f4
Egflam
Peg10
Sorcs3
Abcc12
Pyy
Pgm5
Sytl2
Colgalt2
Higd1a
Galnt13
Igsf21
Mstn
Serpind1
Itih2
Edn3
Col26a1
Ctxn2
Sertm1
Irx1
AF529169
Pdk4
Cdh9
Scin
Sstr2
Avpr1b
Mc4r
Ankrd34c
Fgb
Fam46d
Ugt8a
Hhatl
Arx
Gcg

D

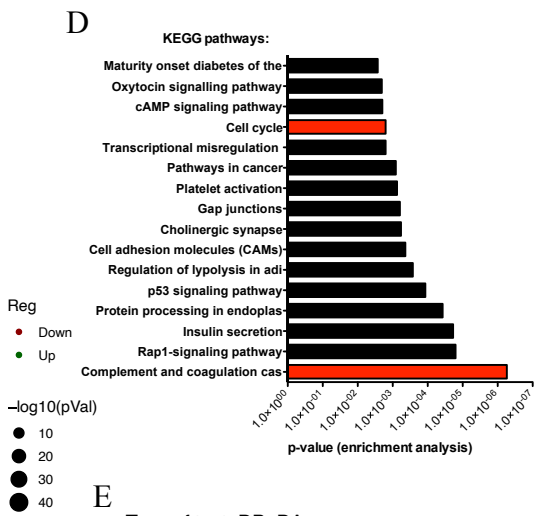
KEGG pathways:
Maturity onset diabetes of the
Oxytocin signalling pathway
cAMP signaling pathway
Cell cycle
Transcriptional misregulation
Pathways in cancer
Platelet activation
Gap junctions
Cholinergic synapse
Cell adhesion molecules (CAMs)
Regulation of lypolysis in adi
p53 signaling pathway
Protein processing in endoplas
Insulin secretion
Rap1-signaling pathway
Complement and coagulation cas
p-value (enrichment analysis)
Reg
Down
Up
−log10(pVal)
10
20
30
40

E

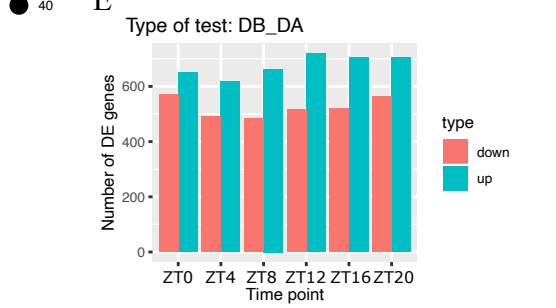
Type of test: DB_DA
Number of DE genes
Time point
ZT0
ZT4
ZT8
ZT12
ZT16
ZT20
type
down
up

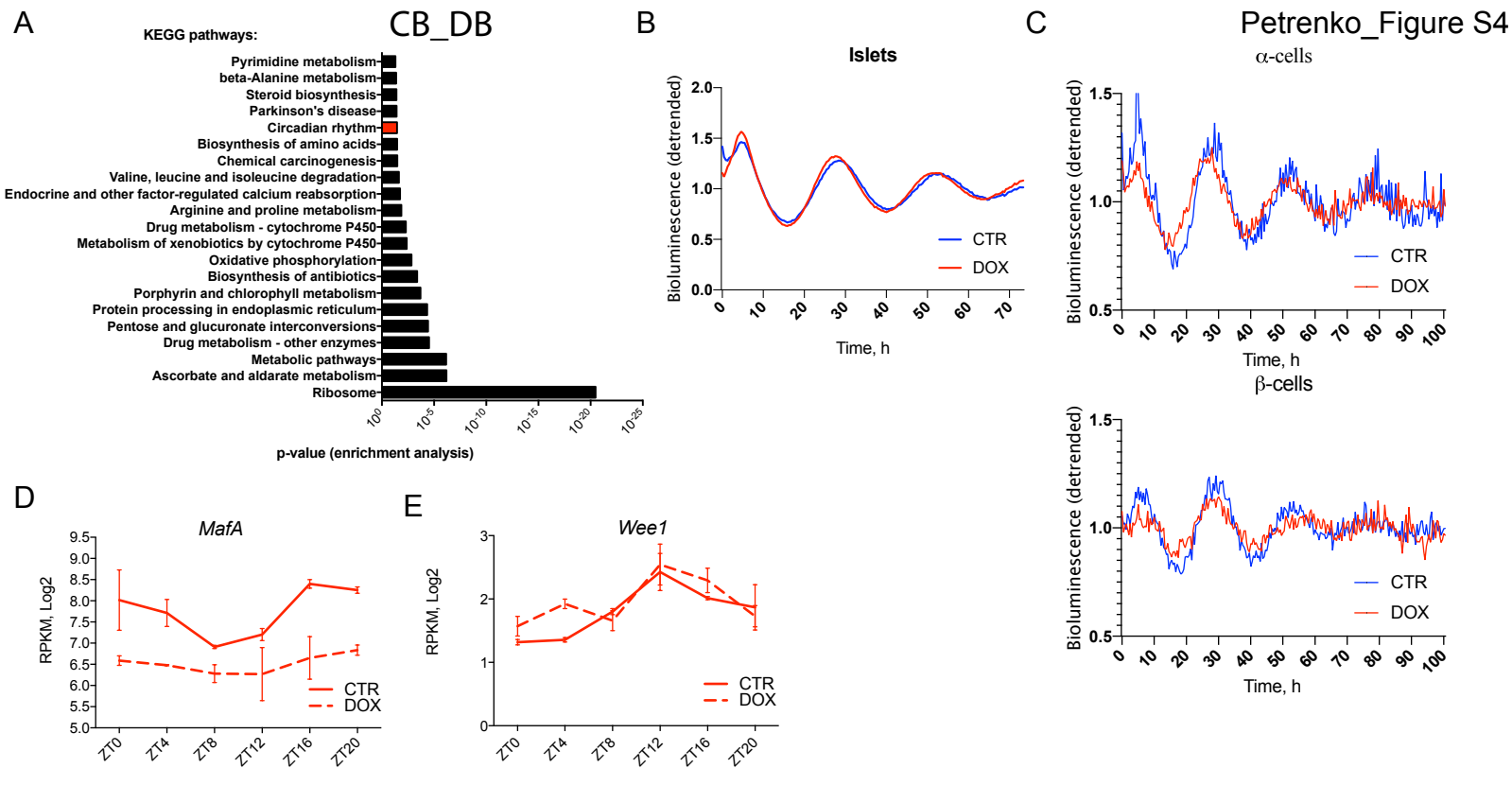
A
CB_DB
KEGG pathways:
Pyrimidine metabolism
beta-Alanine metabolism
Steroid biosynthesis
Parkinson's disease
Circadian rhythm
Biosynthesis of amino acids
Chemical carcinogenesis
Valine, leucine and isoleucine degradation
Endocrine and other factor-regulated calcium reabsorption
Arginine and proline metabolism
Drug metabolism - cytochrome P450
Metabolism of xenobiotics by cytochrome P450
Oxidative phosphorylation
Biosynthesis of antibiotics
Porphyrin and chlorophyll metabolism
Protein processing in endoplasmic reticulum
Pentose and glucuronate interconversions
Drug metabolism - other enzymes
Metabolic pathways
Ascorbate and aldarate metabolism
Ribosome
10^0
10^-5
10^-10
10^-15
10^-20
10^-25
p-value (enrichment analysis)
B
Islets
Bioluminescence (detrended)
2.0
1.5
1.0
0.5
0.0
0
10
20
30
40
50
60
70
Time, h
CTR
DOX
C
Petrenko_Figure S4
α-cells
Bioluminescence (detrended)
1.5
1.0
0.5
0
10
20
30
40
50
60
70
80
90
100
Time, h
CTR
DOX
β-cells
Bioluminescence (detrended)
1.5
1.0
0.5
0
10
20
30
40
50
60
70
80
90
100
Time, h
CTR
DOX
D
MafA
RPKM, Log2
9.5
9.0
8.5
8.0
7.5
7.0
6.5
6.0
5.5
5.0
ZT0
ZT4
ZT8
ZT12
ZT16
ZT20
CTR
DOX
E
Wee1
RPKM, Log2
3
2
1
0
ZT0
ZT4
ZT8
ZT12
ZT16
ZT20
CTR
DOX

A

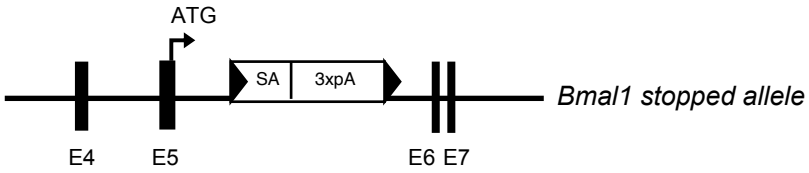
ATG
SA
3xpA
Bmal1 stopped allele
E4
E5
E6 E7

B

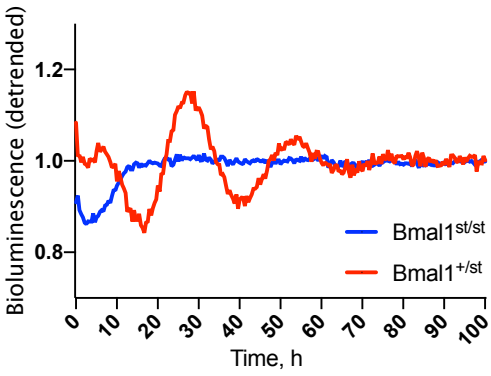
Bioluminescence (detrended)
1.2
1.0
0.8
0
10
20
30
40
50
60
70
80
90
100
Time, h
Bmal1st/st
Bmal1+/st

C

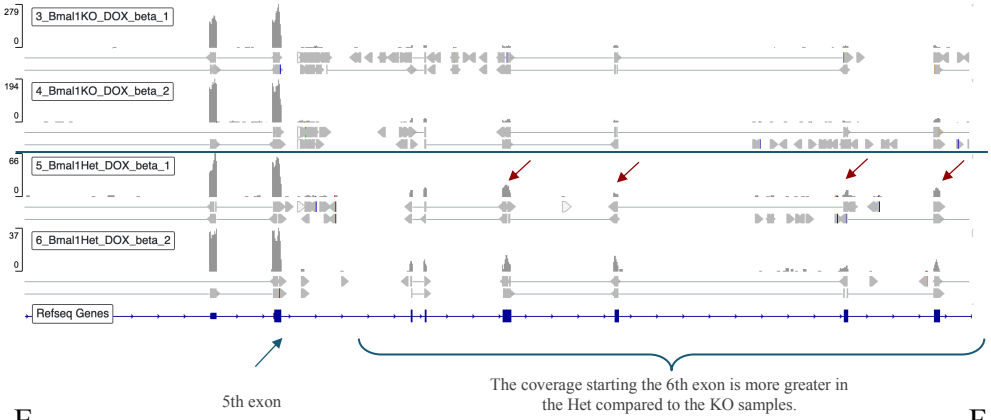
3_Bmal1KO_DOX_beta_1
4_Bmal1KO_DOX_beta_2
5_Bmal1Het_DOX_beta_1
6_Bmal1Het_DOX_beta_2
Refseq Genes
5th exon
The coverage starting the 6th exon is more greater in the Het compared to the KO samples.

D

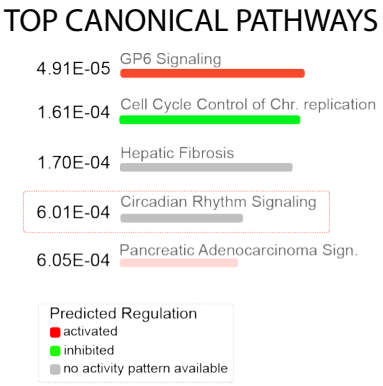
TOP CANONICAL PATHWAYS
4.91E-05 GP6 Signaling
1.61E-04 Cell Cycle Control of Chr. replication
1.70E-04 Hepatic Fibrosis
6.01E-04 Circadian Rhythm Signaling
6.05E-04 Pancreatic Adenocarcinoma Sign.
Predicted Regulation
activated
inhibited
no activity pattern available

E

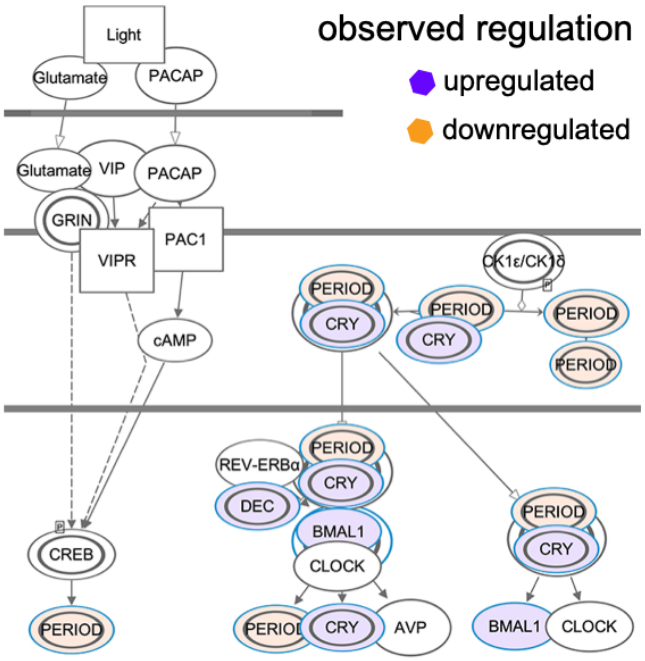
observed regulation
upregulated
downregulated
Light
Glutamate
PACAP
Glutamate
VIP
PACAP
GRIN
VIPR
PAC1
cAMP
CK1ε/CK1δ
PERIOD
CRY
REV-ERBα
DEC
BMAL1
CLOCK
CREB
AVP

F

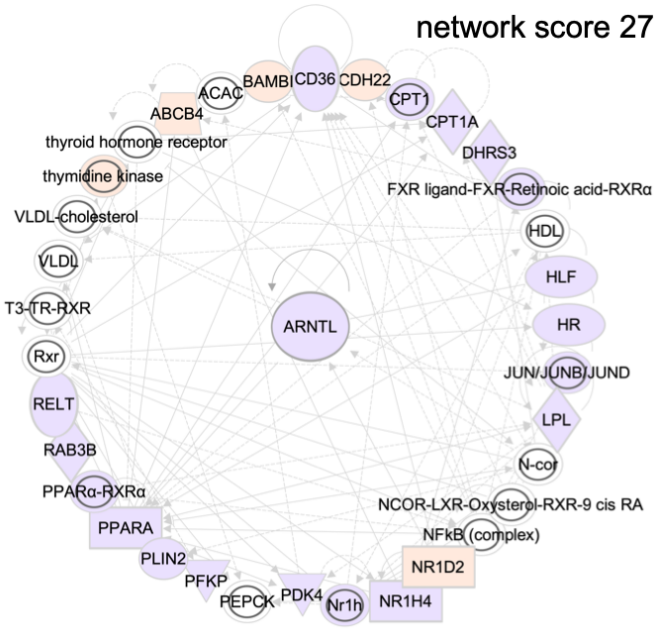
network score 27
BAMBI
CD36
CDH22
ACAC
CPT1
ABCB4
CPT1A
thyroid hormone receptor
DHRS3
thymidine kinase
FXR ligand-FXR-Retnoic acid-RXRα
VLDL-cholesterol
HDL
VLDL
HLF
T3-TR-RXR
ARNTL
HR
Rxr
JUN/JUNB/JUND
RELT
LPL
RAB3B
N-cor
PPARα-RXRα
NCOR-LXR-Oxysterol-RXR-9 cis RA
PPARA
NFkB (complex)
PLIN2
NR1D2
PFKP
PEPCK
PDK4
Nr1h
NR1H4

G

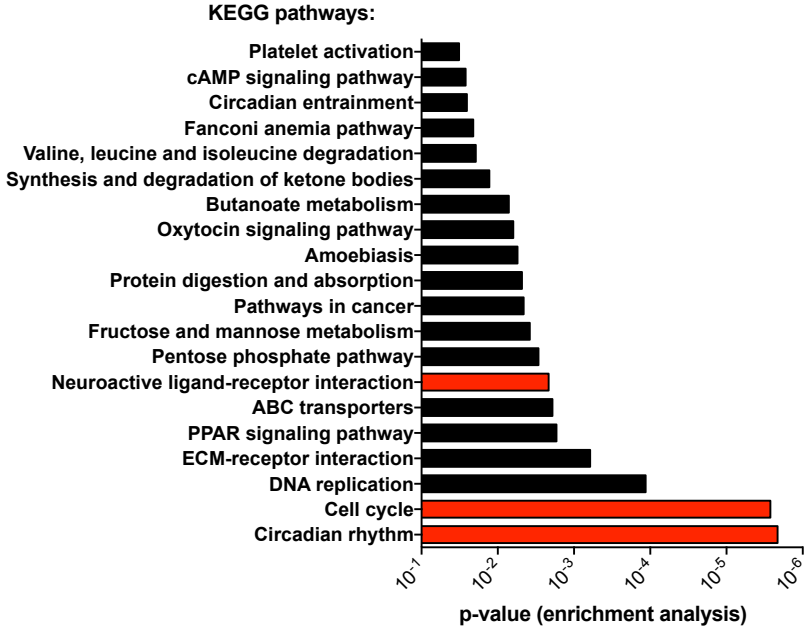
KEGG pathways:
Platelet activation
cAMP signaling pathway
Circadian entrainment
Fanconi anemia pathway
Valine, leucine and isoleucine degradation
Synthesis and degradation of ketone bodies
Butanoate metabolism
Oxytocin signaling pathway
Amoebiasis
Protein digestion and absorption
Pathways in cancer
Fructose and mannose metabolism
Pentose phosphate pathway
Neuroactive ligand-receptor interaction
ABC transporters
PPAR signaling pathway
ECM-receptor interaction
DNA replication
Cell cycle
Circadian rhythm
10-1
10-2
10-3
10-4
10-5
10-6
p-value (enrichment analysis)

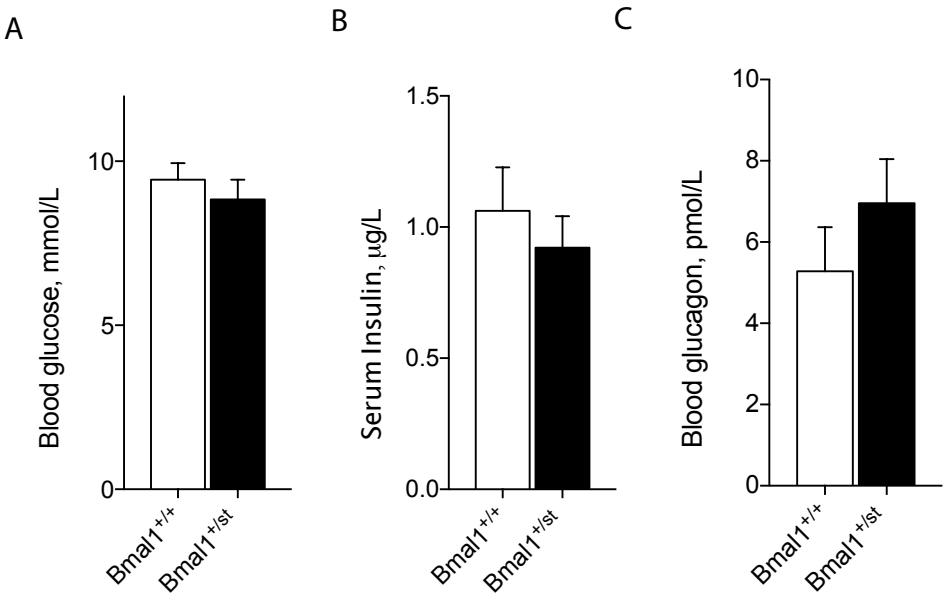
A
Blood glucose, mmol/L
10
5
0
Bmal1+/+
Bmal1+/st
B
Serum Insulin, μg/L
1.5
1.0
0.5
0.0
Bmal1+/+
Bmal1+/st
C
Blood glucagon, pmol/L
10
8
6
4
2
0
Bmal1+/+
Bmal1+/st

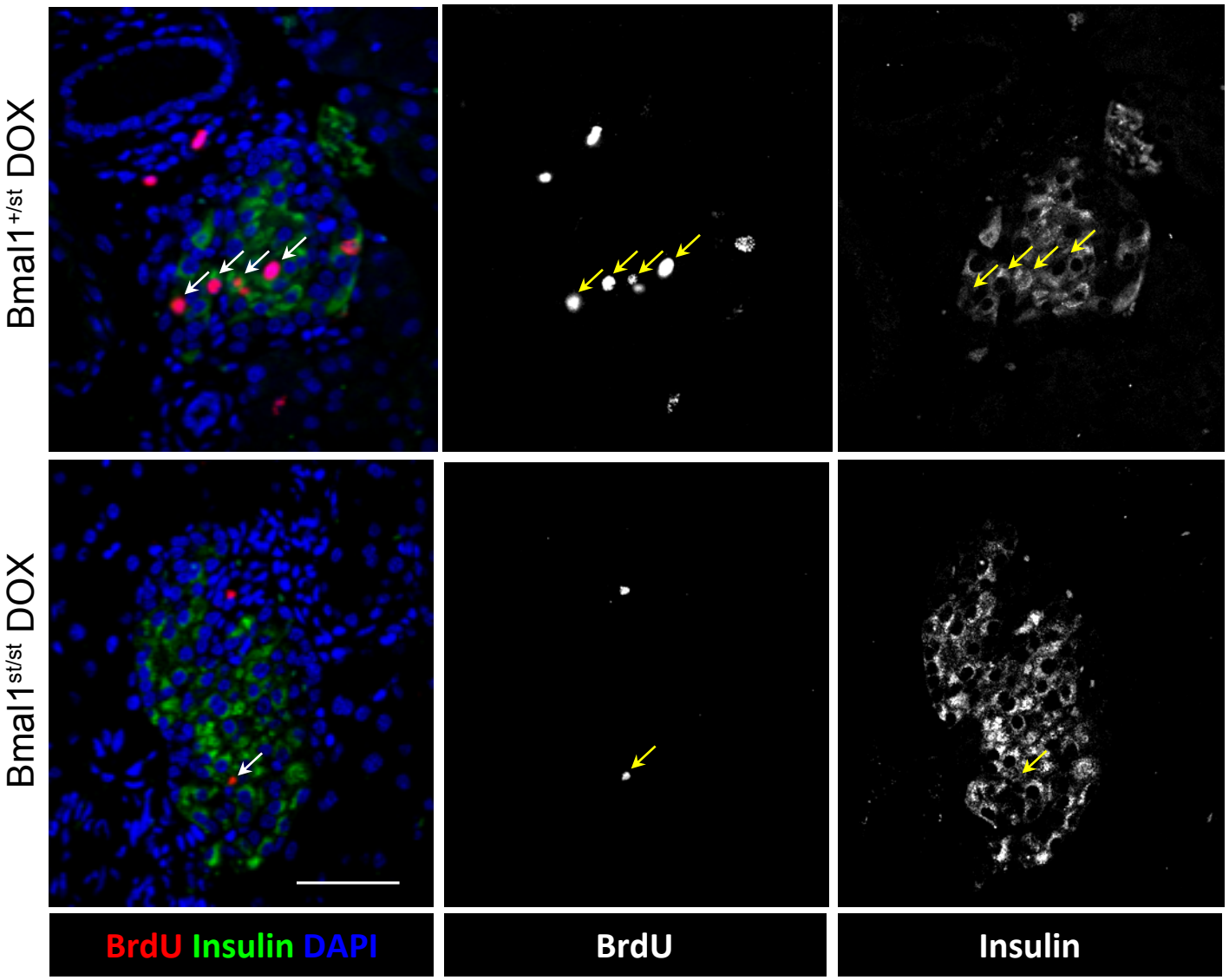
Bmal1+/st DOX
Bmal1st/st DOX
BrdU Insulin DAPI
BrdU
Insulin

Analysis Workflow

Petrenko_Figure S8

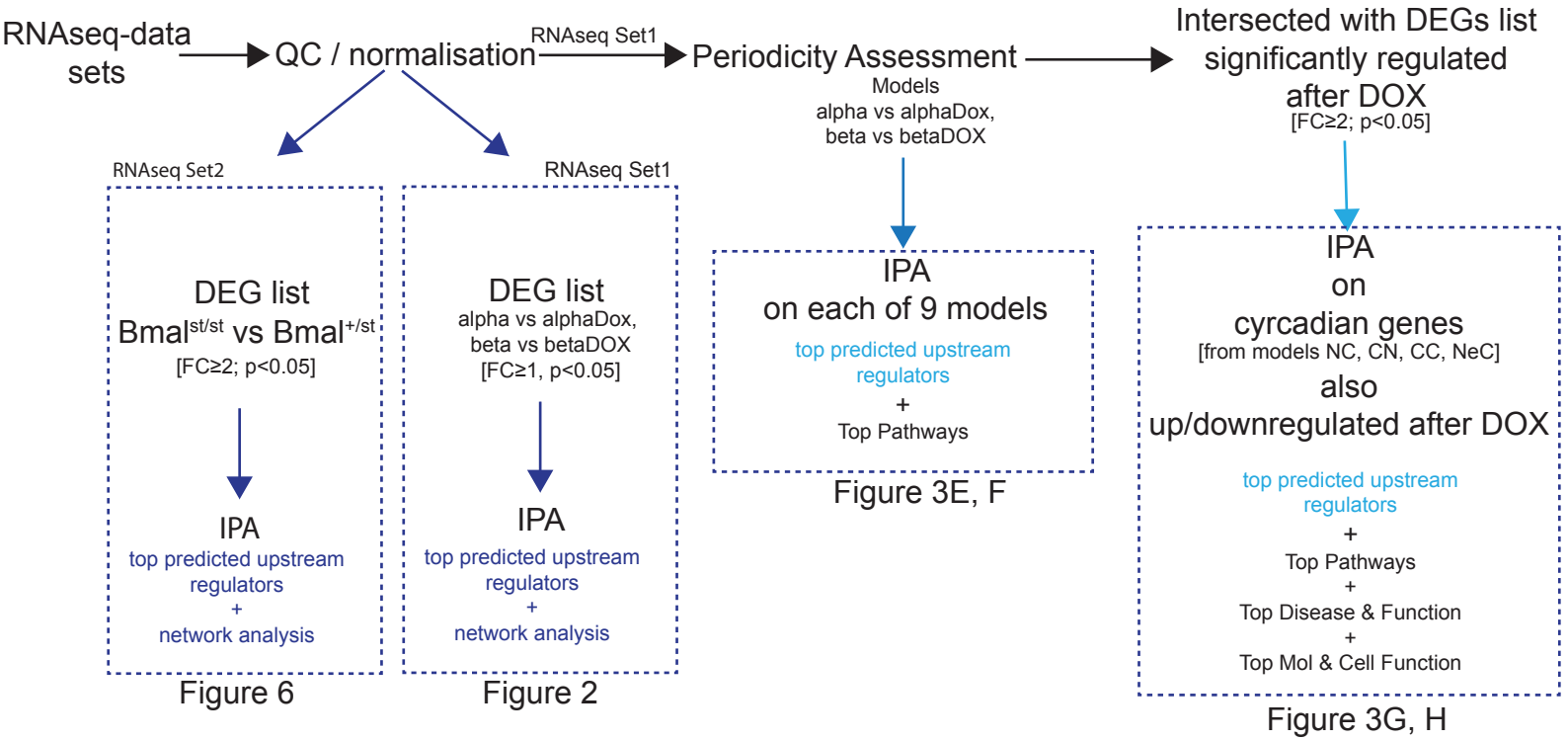

Figure 6

Figure 2

Figure 3E, F

Figure 3G, H